TOXICOLOGICAL SCIENCES **131(2)**, 360–374 2013
doi:10.1093/toxsci/kfs320
Advance Access publication November 9, 2012

Application of an Updated Physiologically Based Pharmacokinetic Model for Chloroform to Evaluate CYP2E1-Mediated Renal Toxicity in Rats and Mice

Alan F. Sasso,*,[1] Paul M. Schlosser,† Gregory L. Kedderis,‡ Mary Beth Genter,§ John E. Snawder,¶ Zheng Li,* Susan Rieth,* and John C. Lipscomb‖

*National Center for Environmental Assessment, Office of Research and Development, U.S. Environmental Protection Agency, Washington, DC 20460; †National Center for Environmental Assessment, Office of Research and Development, U.S. Environmental Protection Agency, Research Triangle Park, NC 27711; ‡Independent consultant, Chapel Hill, NC; §Department of Environmental Health and Center for Environmental Genetics, University of Cincinnati, Cincinnati, OH; ¶Biomonitoring and Health Assessment Branch, Division of Applied Research and Technology, National Institute for Occupational Safety and Health, Centers for Disease Control and Prevention, Cincinnati, OH; and ‖National Center for Environmental Assessment, Office of Research and Development, U.S. Environmental Protection Agency, Cincinnati, OH

[1]To whom correspondence should be addressed at 1200 Pennsylvania Ave, N.W. Mail Code: 8601P Washington, DC 20460. Fax: 703-347-8689. E-mail: sasso.alan@epa.gov.

Received September 14, 2012; accepted November 5, 2012

Physiologically based pharmacokinetic (PBPK) models are tools for interpreting toxicological data and extrapolating observations across species and route of exposure. Chloroform ($CHCl_3$) is a chemical for which there are PBPK models available in different species and multiple sites of toxicity. Because chloroform induces toxic effects in the liver and kidneys via production of reactive metabolites, proper characterization of metabolism in these tissues is essential for risk assessment. Although hepatic metabolism of chloroform is adequately described by these models, there is higher uncertainty for renal metabolism due to a lack of species-specific data and direct measurements of renal metabolism. Furthermore, models typically fail to account for regional differences in metabolic capacity within the kidney. Mischaracterization of renal metabolism may have a negligible effect on systemic chloroform levels, but it is anticipated to have a significant impact on the estimated site-specific production of reactive metabolites. In this article, rate parameters for chloroform metabolism in the kidney are revised for rats, mice, and humans. New *in vitro* data were collected in mice and humans for this purpose and are presented here. The revised PBPK model is used to interpret data of chloroform-induced kidney toxicity in rats and mice exposed via inhalation and drinking water. Benchmark dose (BMD) modeling is used to characterize the dose-response relationship of kidney toxicity markers as a function of PBPK-derived internal kidney dose. Applying the PBPK model, it was also possible to characterize the dose response for a recent data set of rats exposed via multiple routes simultaneously. Consistent BMD modeling results were observed regardless of species or route of exposure.

Key Words: **PBPK; chloroform; kidney; renal toxicity; model.**

Disclaimer: The views expressed in this publication are those of the authors and do not represent the views and policies of their respective agencies. Mention of trade names or commercial products does not constitute endorsement or recommendation for use.

Chloroform ($CHCl_3$) is a trihalomethane present in drinking water as a byproduct of disinfection. It is regulated as a drinking water contaminant by governmental agencies worldwide (Schoeny *et al*., 2006; WHO, 2005). The general population may be exposed to chloroform via ingestion, inhalation, and dermal absorption (Boorman, 1999; Riederer *et al*., 2009). The kidney is one of the established targets of chloroform toxicity in experimental animals. In 2-year studies, renal tubular cytotoxicity and regeneration, characterized by nuclear enlargement of the proximal tubules, dilation of tubular lumen, cytoplasmic basophilia, and tubule hyperplasia, were observed in rats and mice of both sexes exposed to chloroform via inhalation (Yamamoto *et al*., 2002) and in male rats exposed via inhalation and drinking water simultaneously (Nagano *et al*., 2006). Similar effects were observed in a 2-year drinking water study in male rats (Hard *et al*., 2000; Jorgenson *et al*., 1985). The association between chloroform exposure and cytotoxicity and regeneration in kidney tubular cells is supported by findings from short-term oral and inhalation studies in rodents (Kasai *et al*., 2002; Larson *et al*., 1993, 1996; Palmer *et al*., 1979; Roe *et al*., 1979; Templin *et al*., 1996a, b, 1998).

Chloroform toxicity results from the formation of reactive metabolites, as evidenced by *in vivo* and *in vitro* studies in multiple organ systems. Toxicity in the liver, kidneys, and nasal airways associated with chloroform exposure was increased by cytochrome P450 inducers and reduced by inhibitors of microsomal enzymes (Brown *et al*., 1974; Constan *et al*., 1999; Fang *et al*., 2008; Gopinath and Ford, 1975). The degree of toxicity was also correlated with the extent of chloroform metabolism (Smith and Hook, 1983). Variations in response between tissues, sexes, and species generally correlate with differences in

metabolic rates. For example, male mice have been shown to be more susceptible to chloroform-induced renal toxicity than females (Kasai *et al*., 2002; Templin et al., 1996a, 1998), and renal cytochrome P450 levels in mice are increased by testosterone (Henderson *et al*., 1990; Hong *et al*., 1989; Mohla *et al*., 1988). Furthermore, mice have been reported to metabolize chloroform faster than rats (Corley *et al*., 1990) while also exhibiting higher susceptibility to chloroform-induced toxicity (Kasai *et al*., 2002).

Reactive metabolites of chloroform include phosgene and dichloromethyl free radicals. Phosgene is produced by CYP2E1-mediated oxidative metabolism of chloroform, and oxidative metabolism is the predominant metabolic pathway *in vivo* (Testai *et al*., 1996). Phosgene may react with a wide variety of nucleophiles, including primary and secondary amines, hydroxyl groups, and thiols in cellular macromolecules, resulting in the formation of covalent adducts (De Biasi *et al*., 1992; Gemma *et al*., 1996a; Noort *et al*., 2000; Pereira and Chang, 1981; Pereira *et al*., 1984; Pohl *et al*., 1981; Testai *et al*., 1990). Dichloromethyl free radicals are produced via reductive metabolism, primarily by CYP2E1 under anoxic conditions, but may also involve CYP2B and CYP6A at high concentrations (Gemma *et al*., 2003; Testai *et al*., 1996). They are also highly reactive and may form covalent adducts and induce oxidative stress such as lipid peroxidation (De Biasi *et al*., 1992; Gemma *et al*., 1996a, b; Vittozzi *et al*., 2000). At low cellular concentrations of chloroform, renal metabolism is primarily oxidative (Gemma *et al*., 1996a; Smith and Hook, 1984). At high concentrations, renal metabolism varies across different rodent species. Both oxidative and reductive metabolic pathways have been observed in the mouse kidney (Gemma *et al*., 1996b). However, there is greater uncertainty for the rat kidney. Although studies suggested that reductive metabolic pathway predominates in the rat renal cortex, the available data are insufficient to conclude that phosgene or other oxidative metabolites are absent (Gemma *et al*., 1996a, 2004; Vittozzi *et al*., 2000).

Due to the importance of site-specific chloroform metabolism, physiologically based pharmacokinetic (PBPK) models of chloroform have been developed for rats, mice, and humans for multiple routes of exposure (Corley *et al*., 1990; Roy *et al*., 1996). PBPK models describe the absorption, distribution, metabolism, and elimination of chemicals in the body using a series of differential mass balances. Each tissue is typically modeled using an ordinary differential equation that describes the changes in the mass of chemical in the tissue over time (Chiu *et al*., 2007). Equation 1 outlines the mass balance equation for a single compartment (in which metabolism occurs following Michaelis-Menten kinetics), and Figure 1 illustrates the complete PBPK model of chloroform developed in this work.

$$\frac{dA_t}{dt} = Q_t \times (Ca - Cv_t) - \frac{Vmax \times Cv_t}{Km + Cv_t};\ C_t = \frac{A_t}{V_t};\ Cv_t = \frac{C_t}{P_t} \quad (1)$$

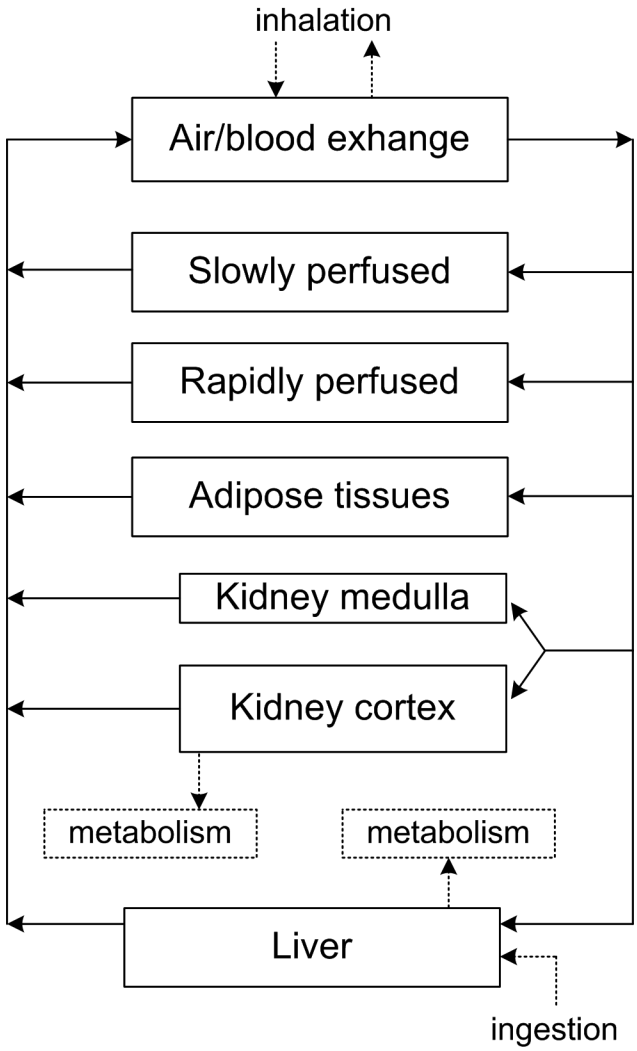

FIG. 1. Flow diagram illustrating a PBPK model of chloroform in rats, mice, and humans.

A_t is amount of chemical in the tissue (mass); Ca is concentration in arterial blood (mass/volume); Cv_t is concentration in venous blood leaving the tissue; C_t is concentration of chemical in the tissue; Q_t is blood flow rate to the tissue (volume/time); V_t is volume of the tissue; P_t is tissue:blood partition coefficient for the chemical in the particular tissue; Vmax is maximal velocity of enzymatic reaction mass/time); and Km is Michaelis-Menten affinity constant (mass/volume).

PBPK models have been used to interpret chloroform-induced organ toxicity data and to simulate potential effects in humans (Evans *et al*., 2002; Liao *et al*., 2007; Luke *et al*., 2010; Meek *et al*., 2002). However, model inconsistencies have arisen due to lack of kidney-specific data and differences in assumptions for relating kidney and liver metabolic rates (i.e., accounting for microsomal protein (MSP) content and the mass of metabolically active region of the kidney). In this article, we improve estimates of renal chloroform metabolism using new

data for CYP450 content in the kidneys of rodents and humans. The modified PBPK model is applied to published toxicological data from rats and mice exposed to chloroform via inhalation or drinking water. Because site-specific kidney metabolism was used as the internal dose metric, it was also possible to evaluate toxicological data for male rats exposed simultaneously via inhalation and drinking water.

MATERIAL AND METHODS

Revision of the PBPK model. The PBPK model by Corley *et al*. (1990) was first revised by dividing the kidney into two compartments, reflecting the physiological difference between the renal cortex and medulla (Aukland, 1976; Barger and Herd, 1973; Navar *et al*., 1983). The model assumes that the renal cortex comprises 70% of the total kidney volume, receives 90% of the blood flow, and expresses 100% of the kidney CYP2E1 activity. The medulla is represented by the remainder of the total volume and blood flow and is assumed to contain no metabolic capacity. This modeling approach has been applied previously by Health Canada to evaluate chloroform-induced renal toxicity (Meek *et al*., 2002).

Kidney cortex metabolic rate constants were revised using species-specific data for CYP2E1 content in the cortex and metabolism of chloroform by CYP2E1. These values were based on measured or derived values for the MSP concentration in tissue (mg protein/g tissue), the tissue mass (g tissue), the CYP2E1 content of the MSP (pmol CYP2E1/mg MSP), and the specific activity of CYP2E1 toward chloroform (pmol chloroform metabolized/min per pmol CYP2E1) (Lipscomb *et al*., 2004; Yoon *et al*., 2007). The inherent activity of CYP2E1 toward chloroform was assumed to be equivalent in both the liver and kidneys. The total metabolic rate constant (VmaxC) in a tissue is the product of these terms with unit conversions, resulting in an unscaled value in units of milligram per hour chloroform metabolized (per $kg^{0.7}$ body weight when allometrically scaled). Kidney cortex metabolic rate ($VmaxC_K$) was estimated as a fraction of the liver metabolic rate ($VmaxC_L$) accounting for underlying tissue differences in the tissue MSP content and the content of CYP2E1 in MSP. The kidney cortex/liver VmaxC ratio can be calculated based on the cortex/liver ratios of three parameters: the joint CYP2E1 content and activity of the tissue MSP, concentration of MSP in tissue, and tissue mass:

$$\frac{VmaxC_K}{VmaxC_L} = \left(\frac{\text{pmol CF metabolized/min/pmol cortex 2E1}}{\text{pmol CF metabolized/min/pmol liver 2E1}} \times \frac{\text{pmol cortex 2E1/mg MSP}}{\text{pmol liver 2E1/mg MSP}}\right) \times \left(\frac{\text{mg MSP/g cortex}}{\text{mg MSP/g liver}}\right) \times \frac{\text{g cortex}}{\text{g liver}} \quad (2)$$

Although the CYP2E1 enzyme activity toward a substrate (in pmol chloroform metabolized/min/pmol CYP2E1) is assumed equal between the liver and kidneys, *in vitro* experiments usually measure the joint activity and CYP2E1 content (i.e., pmol/min/mg MSP).

An earlier relationship for calculating the kidney:liver metabolic ratios (adapted below) was presented by Corley *et al*. (1990):

$$\frac{VmaxC_K}{VmaxC_L} = \frac{[V/S]_K}{[V/S]_L} \times \frac{\text{g kidney}}{\text{g liver}} \quad (3)$$

The parameter [V/S] represents the *in vitro* velocity-to-substrate ratio, and the ratio of kidney:liver [V/S] is defined by Corley *et al*. (1990) as the parameter **A**.

However, Equation 3 leaves out the kidney:liver ratio of milligrams of MSP per gram tissue: the second bracketed term in Equation 2. Because the liver contains higher levels of MSP per gram of tissue, neglecting the ratio of milligrams of MSP in tissues leads to an overestimation of renal metabolism and also neglects a potential source of interspecies variation. Overestimation of metabolism is compounded by the fact that the equation assumes the entire kidney is metabolically active, as opposed to only the kidney cortex.

Collection and analysis of mouse and human tissue data. Limited data are available for human MSP and CYP2E1 content in the kidney. Few studies have quantified CYP2E1 in human kidney because renal levels of CYP2E1 are typically below the limits of detection for gels and blots (Amet *et al*., 1997; Baker *et al*., 2005; Cummings *et al*., 2000). The ELISA technique has proven more sensitive than conventional gels and blots and has produced estimates of human liver MSP CYP2E1 concentrations that are in agreement with estimates based on the other approaches (Snawder and Lipscomb, 2000). Paired human renal cortex and liver samples were available from four female Caucasian donors, and ELISA was conducted as previously described (Davis *et al*., 2002; Snawder and Lipscomb, 2000). Duplicate samples of MSP were analyzed for CYP2E1 content and expressed as pmol CYP/mg MSP. Although these human MSP samples were not originally procured specifically for this work, original research to quantify CYP2E1 content was carried out in NIOSH's Taft Laboratory (Cincinnati, OH) under Investigational Review Board–approved protocols.

There was also a paucity of data available in the mouse kidney to derive the site-specific rate of chloroform metabolism. Two male mice were euthanized by carbon dioxide asphyxiation, and livers and kidneys were removed and weighed. Kidneys were bisected, and the inner portion (medullary region) was isolated from the cortical region based on grossly observable differences in tissue coloration. Tissues were homogenized and MSP isolated by differential centrifugation. The yield of MSP per gram tissue in mice was determined volumetrically by accounting for total protein content and volumes of tissue homogenate and prepared MSP. These animal studies were conducted under a protocol approved by the University of Cincinnati Animal Institutional Care and Use Committee.

RESULTS

Derivation of Human Renal Cortex Chloroform Metabolic Rate

The CYP2E1 content of human renal cortex MSP using the ELISA technique is presented in Table 1. The CYP2E1 content in matched samples of renal cortex and liver MSP indicates that human renal cortex MSP contains approximately 14.5% of that found in the liver.

Because no data were available to estimate the human renal cortex MSP content (mg MSP/gram cortex), the value for MSP content of human liver (32 mg/g liver [Barter *et al*., 2007]) was used; i.e., the cortex:liver MSP content ratio was assumed to be unity. This likely represents an overestimation based on results for rats and mice (which demonstrate ratios of 0.87 and 0.70, respectively) and may cause the human model to overpredict renal metabolism and hence human renal toxicity by an unknown (but health protective) fraction. The kidney cortex:liver VmaxC ratio for the human (0.017) was calculated from the product of the cortex:liver microsomal activity ratio, the cortex:liver MSP concentration ratio, and the ratio of cortex:liver tissue mass:

$$\frac{VmaxC_K}{VmaxC_L} = 0.145 \frac{\text{cortex pmol 2E1/mg MSP}}{\text{liver pmol 2E1/mg MSP}} \times \frac{\text{32 mg MSP/g cortex}}{\text{32 mg MSP/g liver}} \times \frac{\text{0.0044 g kidney/g BW} \times \text{0.7 g cortex/g kidney}}{\text{0.026 g liver/g BW}}$$

The 70% cortex:whole-kidney correction was employed because the CYP2E1 content measurement is cortex specific.

Derivation of Rat Renal Cortex Chloroform Metabolic Rate

Data are available in the literature to derive updated renal metabolic rate parameters in the rat (Cummings *et al*., 1999, 2001; Zerilli *et al*., 1995). The analysis by Yoon *et al*. (2007) produced estimates of both kidney and liver CYP2E1 activity (in nmol/min/mg MSP) and MSP content (in mg/g tissue). Kidney CYP2E1 activity was estimated to be approximately 5% of the liver, whereas MSP content ratio was 87%. The final ratio of kidney cortex/liver VmaxC (0.008) is the product of the MSP ratio, the CYP2E1 activity ratio, and the ratio of whole-organ volumes:

$$\frac{\text{VmaxC}_K}{\text{VmaxC}_L} = \frac{0.036\ \text{nmol/min/mg MSP}}{0.662\ \text{nmol/min/mg MSP}} \times \frac{18.1\ \text{mg MSP/g kidney}}{20.7\ \text{mg MSP/g liver}} \times \frac{0.007\ \text{g kidney/g BW}}{0.04\ \text{g liver/g BW}}$$

As Yoon *et al*. (2007) determined the total CYP2E1 content in the whole kidney, a 70% adjustment for kidney cortex:whole kidney volume was not applied because it would lead to an underestimation of total metabolic capacity of the kidney. The PBPK model, however, will assume that the whole-kidney activity measured *in vitro* is concentrated in the cortex.

Derivation of Mouse Renal Cortex Chloroform Metabolic Rate

The ratio of MSP content (mg MSP/gram tissue) between the kidney cortex and liver for the mouse, determined by the measured recovery of MSP from matched tissue samples from two adult male mice, is presented in Table 2. MSP yields from the two samples were averaged and included in calculations as a point estimate of 14.85 mg MSP/g mouse renal cortex. These results demonstrated that, on a per gram of tissue basis, total MSP in mouse renal cortex was 70% of that of mouse liver.

The CYP2E1 content of mouse renal cortex microsomes has not been directly determined, but some data are available to estimate the CYP2E1 content of mouse renal cortex microsomes relative to liver microsomes. Because the majority of renal CYP2E1 expression has been found in the kidney cortex versus medulla (Lohr *et al*., 1998), observed CYP2E1 metabolic rates from whole-kidney homogenates were attributed to the cortex. In particular, based on Corley *et al*. (1990) measurement of the microsomal metabolism of chloroform at saturating concentrations (0.0102 and 0.0654 nmol/min/mg protein for kidney and liver, respectively), the activity for mouse kidney MSP–mediated chloroform metabolism is assumed to be 15.6% of the corresponding hepatic metabolism.

The values in Table 2 were also employed to correct the observation by Corley *et al*. (1990). The observed microsomal metabolism (0.0102 nmol/min/mg MSP) was determined on a whole-kidney basis and was not cortex specific. If we assume that only the cortex was metabolically active, then this observation was diluted slightly by the existence of MSP from the medulla. Based on the values in Table 2, 77% of whole-kidney MSP originates from the cortex. Therefore, the value 0.0102 nmol/min/mg MSP should be scaled up to 0.0132 nmol/min cortex MSP (i.e., 0.0102/0.77)

The kidney cortex:liver VmaxC ratio for the mouse (0.030) was the product of the whole kidney:liver microsomal activity ratio, the cortex:liver MSP concentration ratio, and the ratio of cortex:liver tissue mass:

$$\frac{\text{VmaxC}_K}{\text{VmaxC}_L} = \frac{0.0132\ \text{nmol/min/mg MSP}}{0.0654\ \text{nmol/min/mg MSP}} \times \frac{14.85\ \text{mg MSP/g cortex}}{21.1\ \text{mg MSP/g liver}} \times \ldots \frac{0.0167\ \text{g kidney/g BW} \times 0.7\ \text{g cortex/g kidney}}{0.055\ \text{g liver/g BW}}$$

A 70% cortex:whole-kidney correction was employed because the microsomal content and activity ratios were specific to the cortex.

Relative to previously published estimates of renal cortex chloroform metabolism, the current values for kidney metabolism are higher for humans, but lower for rodents (Table 3). An increased human kidney VmaxC is not surprising because newer methods have higher sensitivity, and analyzing the cortex (as opposed to the whole kidney) may further enhance the ability to measure CYP2E1. The absolute change in the kidney VmaxC from prior estimates is moderate for all three species. However, small differences in kidney metabolic rate for humans relative to rodents can have a significant impact on cross-route extrapolation. All PBPK parameters used in this study are listed in Table 4, and model codes are provided as supplementary materials.

TABLE 1
ELISA-Determined CYP2E1 Content of MSP From Paired Human Renal Cortex and Liver Samples

Human donor[a]	Liver[b]	Renal cortex[b]	Cortex/Liver
013197-1	122	22	0.18
090997-1	41	5.5	0.13
012598-1	31	5.0	0.16
030798-2	30	6.7	0.11
Mean	56	9.8	0.145

[a]All donors were Caucasian females.
[b]Data expressed as picamoles of CYP2E1 per millligrams MSP.

TABLE 2
MSP in Mouse Liver and Kidney

	Cortex 1	Cortex 2	Medulla 1	Medulla 2	Liver 1	Liver 2
Tissue weight (g)	0.295	0.318	0.051	0.055	1.46	1.76
MSP volume (ml)	0.200	0.200	0.100	0.100	0.200	0.200
MSP content (mg/ml)	11.1	13.7	3.3	6.0	18.7	16.3
Yield MSP (mg)	2.22	2.74	0.33	0.60	3.74	3.26
MSP/gram tissue	14.7	15.0	7.8	12.6	24.4	18.0

TABLE 3
Estimates of $VmaxC_K$ (mg/h-kg$^{0.7}$) Across Different Studies and Species

Reference	Rat	Mouse	Human
Corley *et al.* (1990)[a]	0.099	1.012	0.073
Liao *et al.* (2007)[a]	0.081	1.193	0.054
Meek *et al.* (2002)	0.067	—	0.089
Current	0.042	0.684	0.154

[a]Values calculated from Equation 3, while using study-specific physiological and biochemical parameters.

TABLE 4
PBPK Model Parameters for Chloroform

Parameter[a]	Rat	Mouse	Human
BW (kg)	0.25	0.025	70
QPC (vent. rate, l/h/kg$^{0.74}$)	14	23	15
QCC (cardiac output, l/h/kg$^{0.74}$)	14	23	15
QLC (liver blood flow)	0.25	0.25	0.26
QFC (fat blood flow)	0.09	0.09	0.05
QKC (total kidney blood flow)[b]	0.141	0.091	0.18
QSC (slowly perfused flow)	0.15	0.15	0.19
VLC (fraction liver)	0.04	0.055	0.026
VFC (fraction fat)	0.07	0.1	0.19
VKC (fraction kidney)[c]	0.0073	0.0167	0.0044
VSC (slowly perfused)	0.813	0.72	0.63
PL (liver/blood partition)	1.0	0.7	1.6
PF (fat/blood partition)	19.9	10.04[d]	31.0
PK (kidney/blood partiton)[d]	0.62	0.456	0.97
PS (slow/blood partition)	1.0	0.54[d]	1.5
PR (rapid/blood partition)[e]	1.0	0.7	1.6
PB (blood/air partition)	17.7	24.1	11.34[e]
VmaxC (liver, mg/h/kg$^{0.7}$)	5.218	22.8[d]	8.956
VmaxC (kidney, mg/h/kg$^{0.7}$)[f]	0.0417	0.684	0.154
KM (liver, kidney, mg/l)	0.12	0.352[d]	0.012
KRESYN[d]	0	0.125	0
KLOSS[d]	0	5.72e−4	0
Oral absorption (water, h^{-1})	5	5	5
Oral absorption (corn oil, h^{-1})	0.6	0.6	0.6

[a]All values are from Brown *et al.* (1997) and Lipscomb and Kedderis (2006), unless otherwise noted.
[b]Cortex = 0.9 QKC; Medulla = 0.1 QKC.
[c]Cortex = 0.7 VKC; Medulla = 0.3 VKC.
[d]Corley *et al.* (1990).
[e]Tan *et al.* (2003).
[f]Calculated using a species-specific fraction of liver VmaxC.

Model Verification

The revised PBPK model was developed in the Advanced Continuous Simulation Language using acslXtreme software (Aegis Technologies, Huntsville, AL). The revised model was first tested using identical assumptions as the original Corley PBPK model (Corley *et al.*, 1990). The model was able to reproduce the original results for simulations of data for chloroform uptake, exhalation and tissue deposition from open and closed-chamber inhalation data for chloroform in rodents (Corley *et al.*, 1990), drinking water data in human volunteers (Fry *et al.*, 1972), and oral gavage data in rodents (Brown *et al.*, 1974). Deviation from the original Corley model only became apparent after incorporating the revised physiological and metabolic parameters (Fig. 2), particularly for human oral exposure (Table 5). However, the model still provided adequate fits to the data given uncertainties and interindividual variability. Human hepatic CYP2E1 is known to vary significantly between individuals (i.e., fivefold) and impact liver metabolism (Lipscomb *et al.*, 2003). Predictions presented here remained within twofold of the data.

To further investigate the differences between the current and previous models, the current model was run using physiological parameters employed in the original Corley model (Corley *et al.*, 1990) while maintaining the updated metabolic parameters. Because the resulting predictions were nearly identical to those of the original model (not shown), it can be concluded that most of the difference in fits to the pharmacokinetic data could be attributed to revisions made to underlying physiological parameters (i.e., tissue volumes and blood flow rates). Changes in kidney metabolism, while having a significant impact on the internal dose metric, have a negligible effect on body burden, blood concentrations, and biomarker predictions.

Since the time of the original model development (Corley *et al.*, 1990), additional data have become available. Chloroform tissue concentrations for rats exposed to chloroform via inhalation, drinking water, and both routes simultaneously were generously provided by the Japan Bioassay Research Center (Take *et al.*, 2010) and were simulated using the revised model. Data for kidney, liver, blood, and adipose tissue concentrations in male rats by Take *et al.* (2010) are consistent with model predictions for all pathways (Fig. 3).

Due to nonlinearities related to first-pass metabolism, it was found that the kidney dose metric is highly sensitive to the oral exposure profile. If it is assumed a daily oral dose occurs continuously over 24 h at low levels, the fraction of total metabolism predicted to occur in the liver is relatively high, and the corresponding fraction predicted in the kidney (i.e., the kidney internal dose) is low. Alternatively, if the same average daily oral exposure occurs as discrete bolus dose events occurring a few times a day, there are higher peak concentrations in the liver. This results in an increased saturation of liver metabolism, increased systemic distribution of chloroform, and ultimately a higher kidney dose. The impact of these two alternative oral dose assumptions is presented in Figure 4.

Dose-Response Analysis

Three data sets showing dose-related changes in the kidneys of chloroform-exposed rodents (Hard *et al.*, 2000; Nagano *et al.*, 2006; Yamamoto *et al.*, 2002) were utilized for dose-response analysis. These studies were chosen because they exposed rodents for 2 years, examined kidney toxicity endpoints, and contained enough dose groups for an adequate dose-response analysis. PBPK simulations of the bioassays reproduced experimental conditions using available study data

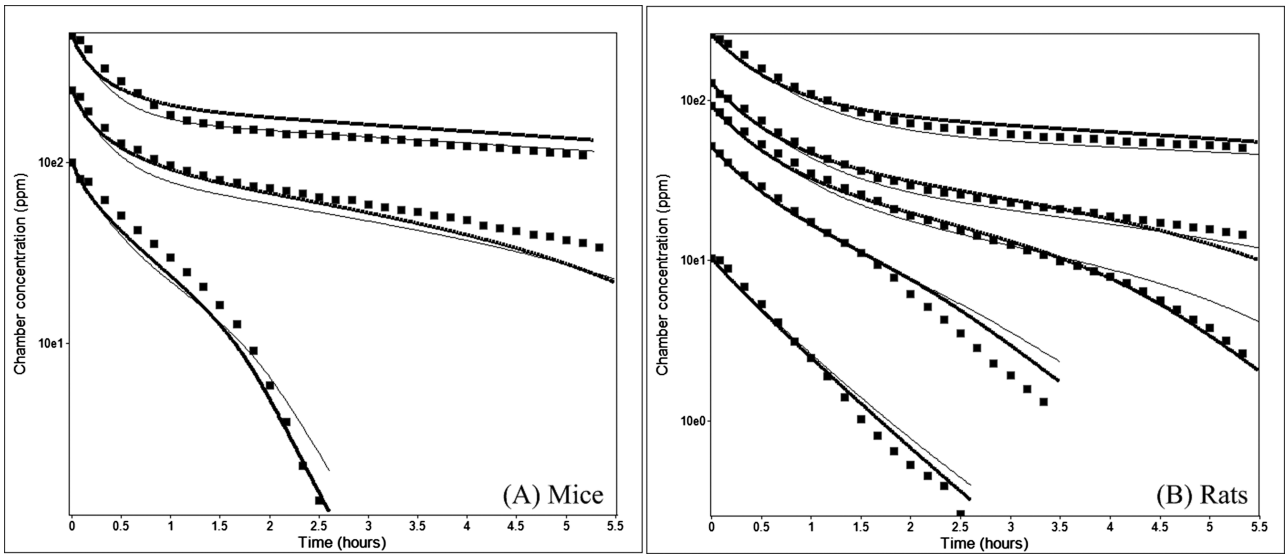

FIG. 2. Comparison of closed-chamber simulations with gas uptake data for mice (A) and rats (B). Simulations using the Corley assumptions (thick lines) and revised assumptions (thin lines) are compared with experimental data (markers).

TABLE 5
Results From Oral and Inhalation Studies in Mice, Rats, and Humans

			Total metabolized (mg)			Total exhaled (mg)		
Route	Species	ppm or mg/kg	Obs.	Corley[a]	Present[b]	Obs.	Corley[a]	Present[b]
Inhalation	Mouse[c]	9.6	0.22	0.46	0.38	0.001	5.8e−4	7.6e−4
		88.8	2.14	3.99	3.39	0.012	0.011	0.011
		366.3	6.76	6.17	5.94	0.62	0.42	0.62
	Rat[c]	93.4	12.10	13.41	12.84	0.25	0.21	0.29
		356	19.40	22.74	21.19	4.87	4.23	6.60
		1041	35.03	30.79	29.93	25.88	26.83	38.94
Oral	Mouse[d]	60	1.40	1.47	1.47	0.10	0.03	0.03
	Rat[d]	60	11.84	10.07	9.74	3.16	4.93	5.26
	Human[e]	7.14	268.8	306.5	325.6	221.2	170.3	156.9
		15.4	317.2	502.3	570.5	646.8	440.1	387.6

Obs = Observed.
[a]Applying Corley PBPK parameters.
[b]Applying updated physiological and metabolic assumptions.
[c]Corley *et al*. (1990).
[d]Brown *et al*. (1997).
[e]Fry *et al*. (1972).

(including study-specific body weights and estimated exposure profiles).

For periodic exposures, the 24-h average dose metric was calculated based on a complete exposure cycle (i.e., for repeated exposures 5 days/week, the calculation was averaged over 7 days).

Because both the Yamamoto *et al*. (2002) and Nagano *et al*. (2006) studies were performed at the same research center and analyzed common endpoints in the same strain of male rat (F344), the data for male rats from the two studies were combined. For the Yamamoto/Nagano studies, inhalation exposure occurred for 6 h/day, 5 days/week and at concentrations between 5 and100 ppm. In the oral component of the Nagano *et al*. (2006) study, rats were administered chloroform in drinking water at a concentration of 1000 ppm (wt/wt); subgroups of these rats were also exposed to chloroform by inhalation at concentrations up to 100 ppm. The pooled incidence data for kidney histopathologic lesions in rats and mice exposed via inhalation, and the estimated PBPK-derived internal dose metrics, are provided as supplementary materials (Supplementary table S-1). The internal dose metrics were also calculated for the multiroute dose groups, and these data were pooled with the inhalation data for male rats (Table 6). An additional 2-year drinking water study in male OM rats by Hard *et al*. (2000) was analyzed separately because of strain and study design differences (Supplementary table S-2).

As mentioned previously, the first-pass effect and choice of simulated oral exposure patterns significantly impacted the estimated internal kidney dose. Because the assumption of

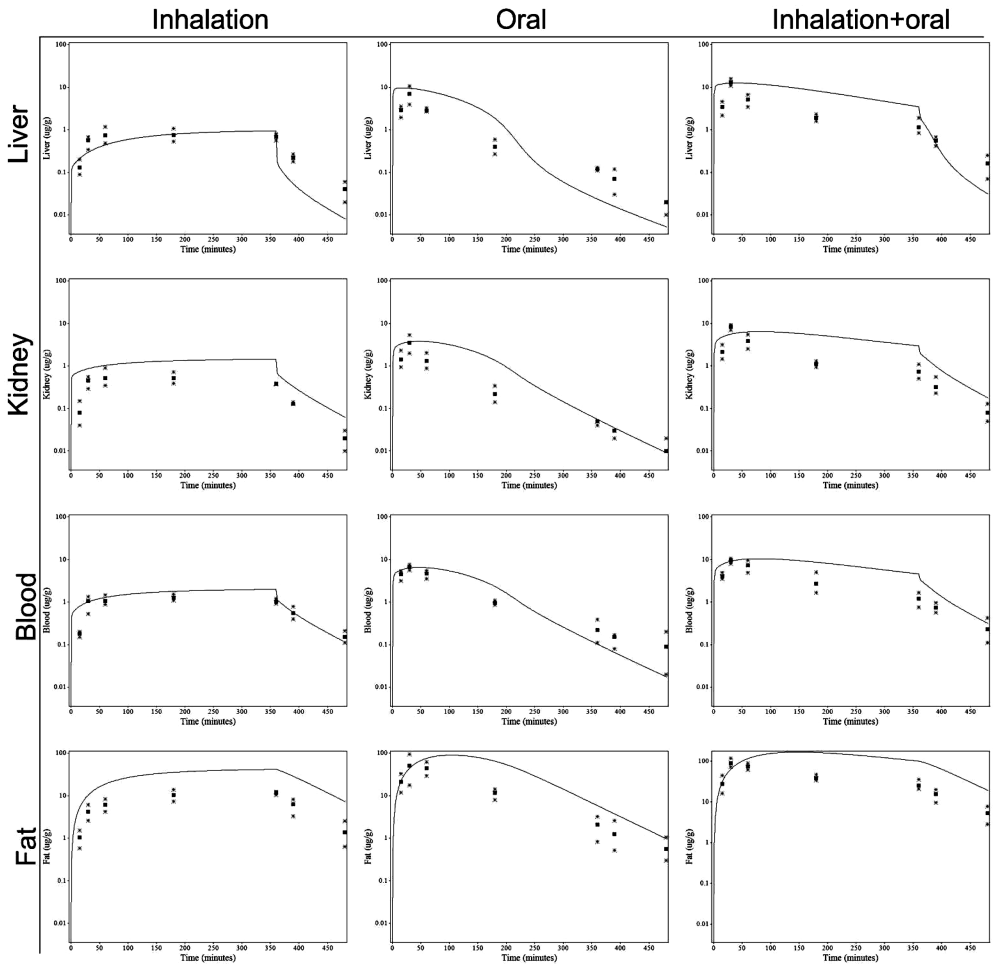

FIG. 3. Comparison of tissue concentration data and model predictions (μg/g tissue) for male rats exposed to either 100 ppm chloroform for 360 min, a single 55 mg/kg oral gavage dose, or both of these exposures simultaneously (Take *et al.*, 2010). Squares indicate the median of five rats. Stars indicate the minimum and maximum measured values.

ingestion in multiple discrete events better matches actual ingestion patterns, PBPK model simulations of chloroform exposure via drinking water in rodents applied the water consumption model by Spiteri (1982). Figure 5 illustrates the impact on the internal dose-response curve for tubular dilation when assuming a continuous 24 h/day oral dose versus sporadic daily doses, employing the Spiteri model. If assuming continuous exposure, the drinking-water data point becomes an outlier because the internal dose metric is underpredicted. Furthermore, if simply analyzing multiroute toxicological data with respect to total absorbed dose, the estimated dose response is nonmonotonic and highly discontinuous.

The benchmark dose (BMD) methodology is routinely used by regulatory agencies to perform quantitative dose response on animal data for human health risk assessment (Davis *et al.*, 2011). This is considered preferable to selecting a no- or lowest observed adverse effect level (NOAEL or LOAEL) because it makes use of all or most of the points in the dose-response data set and is thought to provide results that are less dependent on the dose spacing in the bioassay. Therefore, BMD modeling using the U.S. EPA's BMDS software version 2.1.2 (available at http://www.epa.gov/ncea/bmds) was used to characterize the dose-response relationships for kidney toxicity endpoints in mice and rats. Given a specified benchmark response (BMR) (e.g., a 10% increase in extra risk), an optimal dose-response curve was used to estimate the BMD (the dose that yields the BMR) and the BMDL (the lower confidence limit on the BMD) (U.S. EPA, 2012). A BMR of 10% was applied for all kidney toxicological endpoints. The site-specific 24-h amount of chloroform metabolized (in mg/l-24 h; averaged over 7 days) was used as the internal dose metric for BMD modeling (Evans *et al.*, 2002). For comparison, BMD modeling was also applied using the external exposure (i.e., inhaled air ppm or mg/kg-day oral dose).

Human PBPK model predictions were compared to the internal $BMDL_{10}$ values estimated in rats and mice to predict the human equivalents (human equivalent concentration for the inhalation route, HEC; human equivalent dose for the oral route, HED) for renal effects following exposure to chloroform. The human equivalent exposure is the daily exposure predicted

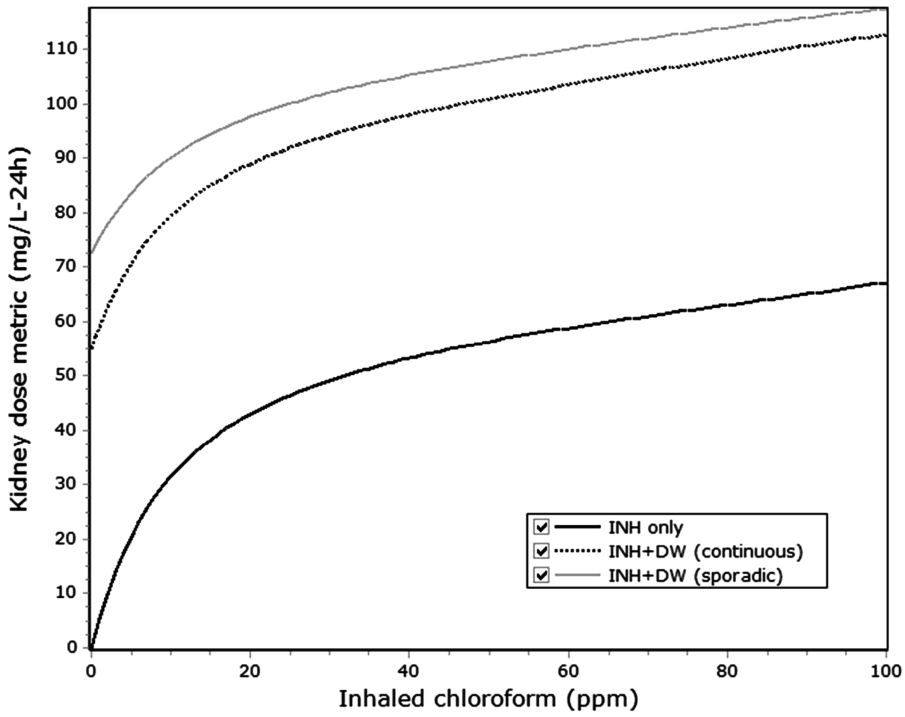

FIG. 4. Comparison of the internal kidney dose metric for rats exposed to chloroform under varying exposure scenarios. INH only indicates rats were exposed to chloroform via inhaled air only (6 hday, 5 days/week). INH+DW indicates rats were exposed via inhaled air and drinking water (50 mg/kg-day oral dose). For the continuous case, it was assumed the drinking water exposure occurred continuously for 24 h per day. For the sporadic case, it was assumed 50 mg/kg-day was distributed as discrete drinking events throughout the day according to the water consumption model by Spiteri (1982).

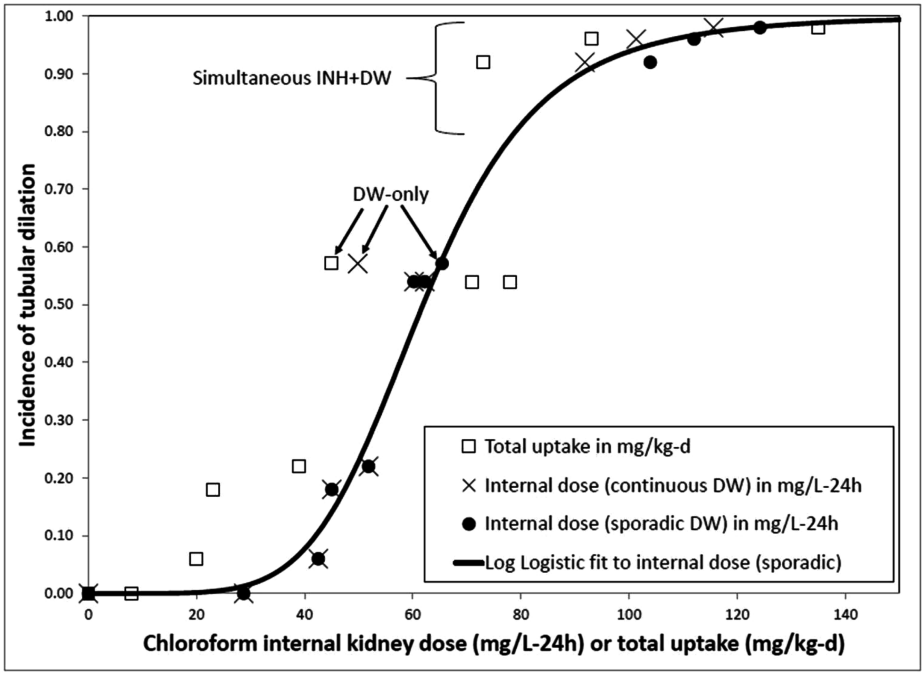

FIG. 5. Dose-response relationship for dilation of the tubular lumen in kidneys of male rats using data from inhalation and multiroute data sets (Table 7, and Supplementary table S-1) (Nagano *et al*., 2006; Yamamoto *et al*., 2002). Response is presented on the basis of total chloroform uptake (estimated by the study authors) and the internal kidney dose metric. Unless noted, data originate from groups of rats exposed via the inhalation pathway only. INH+DW indicates data from the three groups exposed via drinking water and inhalation simultaneously, whereas DW indicates the group exposed via drinking water only. Drinking water was modeled either as occurring continuously 24 h/day (denoted "continuous DW") or according to the model by Spiteri (1982) (denoted "sporadic DW").

TABLE 6
Incidences of Kidney Effects in Male F344 Rats Exposed to Chloroform via Inhalation and Drinking Water Ingestion for 104 Weeks

Dose/Endpoint	Incidence										
Concentration in air (ppm)	0[a,b]	10[a]	25[b]	30[a]	50[b]	90[a]	100[b]	0[b]	25[b]	50[b]	100[b]
Oral dose (mg/kg-day)	0	0	0	0	0	0	0	45	53	54	57
Internal dose[c]	0	28.7	42.5	45.0	51.8	60.2	62.2	65.4	103.9	112.0	124.2
Uptake (mg/kg-day)[d]	0	8	20	23	39	71	78	45	73	93	135
Nuclear enlargement of proximal tubules	0/100	0/50	0/50	5/50	6/50	32/50	33/50	0/49	34/50	47/50	50/50
Dilation of tubular lumen	0/100	0/50	3/50	9/50	11/50	27/50	27/50	28/49	46/50	48/50	49/50
Cytoplasmic basophilia	0/50	—	3/50	—	7/50	—	8/50	9/49	26/50	35/50	36/50
Tubule hyperplasia	1/50	—	0/50	—	0/50	—	0/50	2/49	4/50	7/50	15/50

[a]Yamamoto *et al*. (2002).
[b]Nagano *et al*. (2006).
[c]Average 24-h mg/l tissue chloroform metabolized.
[d]Total absorbed chloroform estimated using methods applied by study authors.

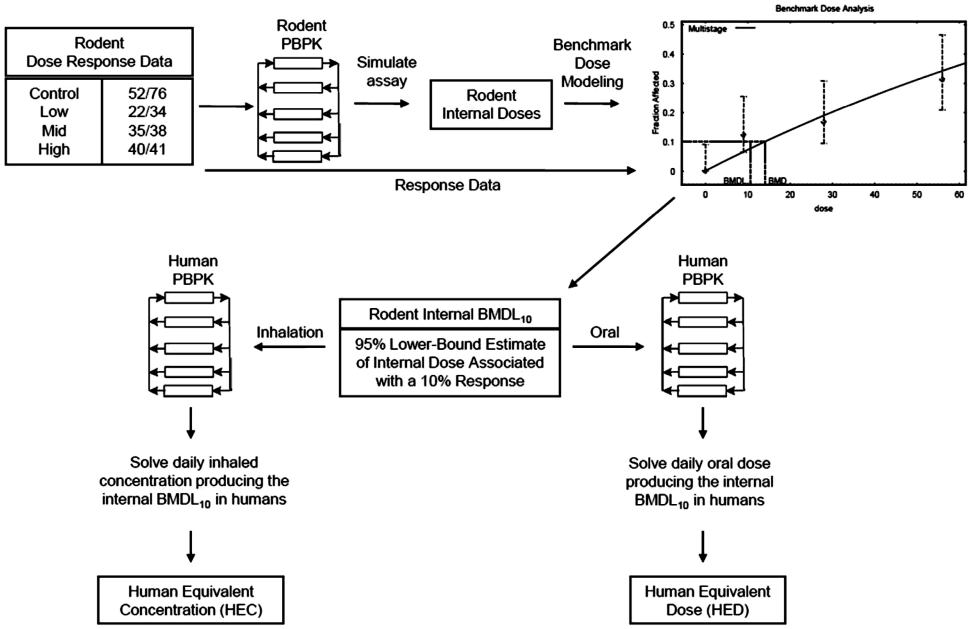

FIG. 6. Process for deriving human equivalent exposures using rodent and human PBPK models. The HEC is the inhaled concentration (in ppm) for which chronic human exposure is predicted to achieve an internal dose that is equal to a predetermined value in the rodent (i.e., an internal kidney $BMDL_{10}$). The HED is the chronic oral dose (in mg/kg-day) predicted to achieve a defined rodent internal dose.

to result in a human internal dose metric equal to the corresponding rodent dose metric at the selected point along the dose-response curve. The human PBPK model also facilitated a route-to-route extrapolation for renal effects from chloroform because human equivalent exposures can be calculated for both oral and inhalation routes regardless of the animal exposure (Fig. 6).

Calculation of the HEC utilizes the assumption of a continuous inhalation exposure, but some special considerations are required for oral exposures. Although breathing occurs continuously through the day and an inhaled agent might be assumed to be encountered at relatively constant concentrations (or not), consumption of drinking water typically occurs as discrete events. Exposure of the human to environmental contaminants via the oral route occurs neither as a bolus event nor as a strictly continuous event. This is important because of the nonlinearities in first-pass metabolism that cause the kidney dose metric to be sensitive to the oral exposure profile. Therefore, simulations for humans exposed to chloroform via drinking water assumed that the daily dose was distributed into six ingestion events where: (1) 25% of the daily dose is ingested at 7 a.m., noon, and 6 p.m., (2) 10% is ingested at 10 a.m. and 3 p.m., and (3) 5% is ingested at 10 p.m. This is clearly an idealized pattern, with actual ingestion patterns expected to vary considerably among individuals and from day to day for each person. Therefore, the sensitivity of model predictions to this pattern was also investigated. It was found that when varied over a reasonable range, the number of ingestion events, and percent distribution, had

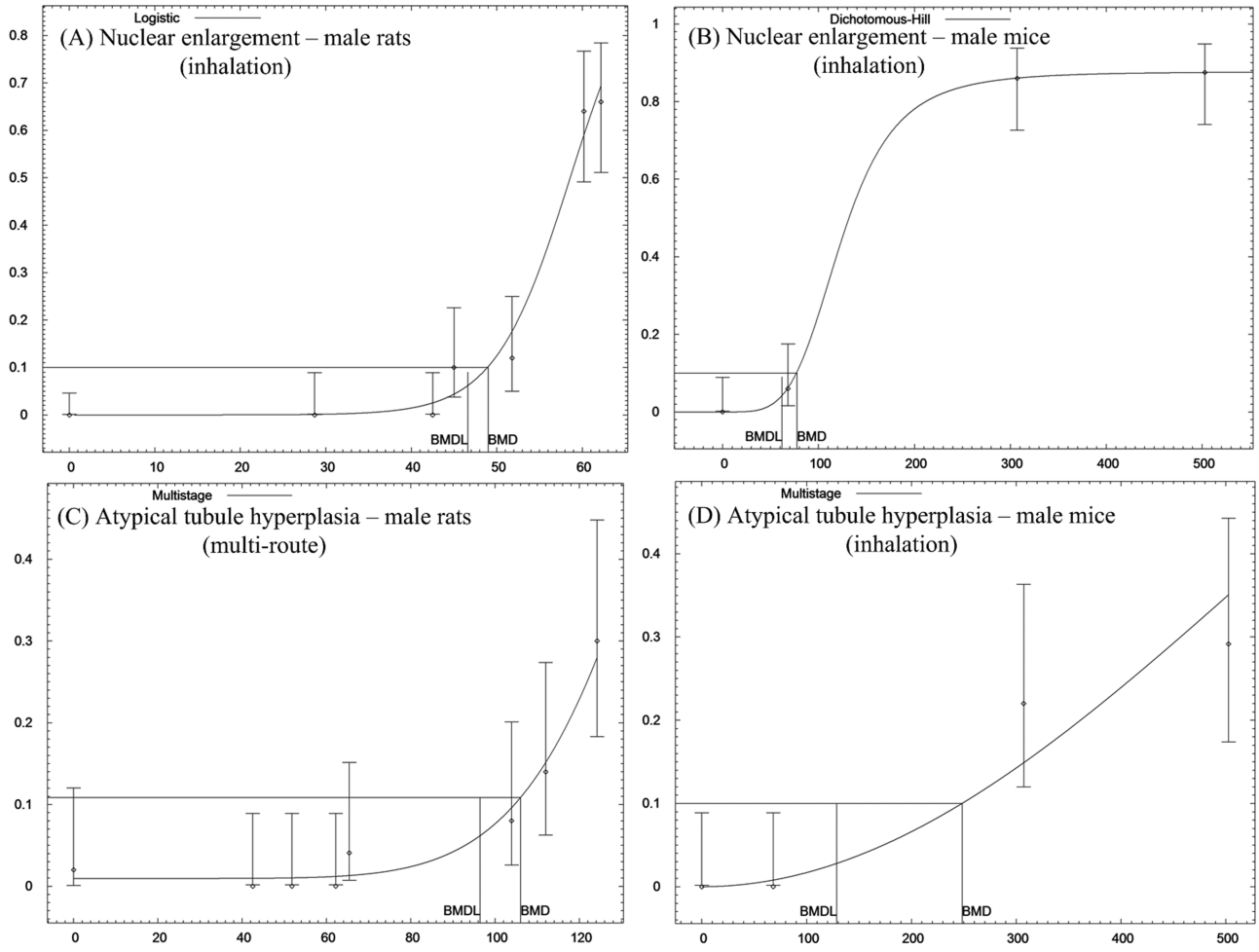

FIG. 7. BMD analysis of two endpoints (nuclear enlargement of proximal tubules and atypical tubule hyperplasia) in male rats and mice using PBPK-derived internal dose metrics using Yamamoto/Nagano data (Nagano *et al*., 2006; Yamamoto *et al*., 2002). The y-axis is fractional incidence of response, and the x-axis is internal kidney dose (mg/l-24 h). Despite differences in susceptibility when the data are examined on a basis of inhaled concentration, the internal $BMDL_{10}$ values for each of the endpoints are relatively close for rats and mice. (A) Nuclear enlargement—male rats (inhalation); (B) nuclear enlargement—male mice (inhalation); (C) atypical tubule hyperplasia—male rats (multiroute); (D) atypical tubule hyperplasia—male mice (inhalation).

only modest impacts on the HED, compared with the difference between assuming continuous ingestion and the idealized pattern. Although oral ingestion can best be simulated using a more complex human exposure model, the pattern assumed here is used to illustrate the effect of applying an assumption other than a baseline continuous daily ingestion. This was also done to maintain some consistency with the rodent intake assumption, which was found to have a strong impact on internal dose. For comparison, a baseline human equivalent dose assuming continuous 24 h/day ingestion (denoted HED_{24}) was calculated. The results of all cross-species and route-to-route extrapolations are presented in Table 7 and as supplementary material (Supplementary table S-3).

DISCUSSION

Although renal toxicity has been determined to be a hazard associated with chloroform exposure across multiple species, quantification has proven difficult due to a high degree of species and route-to-route variations in response. Based on the inhaled concentrations of chloroform required to induce kidney toxicity, mice exhibited higher susceptibility than rats and were also more prone to acute lethality (Philip *et al*., 2006; Yamamoto *et al*., 1999, 2002). The significant contribution of this work is that, with the revision of estimated renal metabolism to be more consistent with (newly) available data and subsequent prediction of the internal target doses with a PBPK model, it is possible to harmonize these databases that previously appeared to be inconsistent. When the measure of dose was changed from inhaled concentration to the renal dose metric, it became evident that rats and mice demonstrate similar levels of response, indicating that rat-mouse species differences in response may be mediated more by toxicokinetic differences than toxicodynamic differences. Evaluating the commonly studied endpoint of nuclear enlargement of the proximal tubule, it can be seen that although mice demonstrate a higher response rate than rats when assessed by inhaled concentration, this

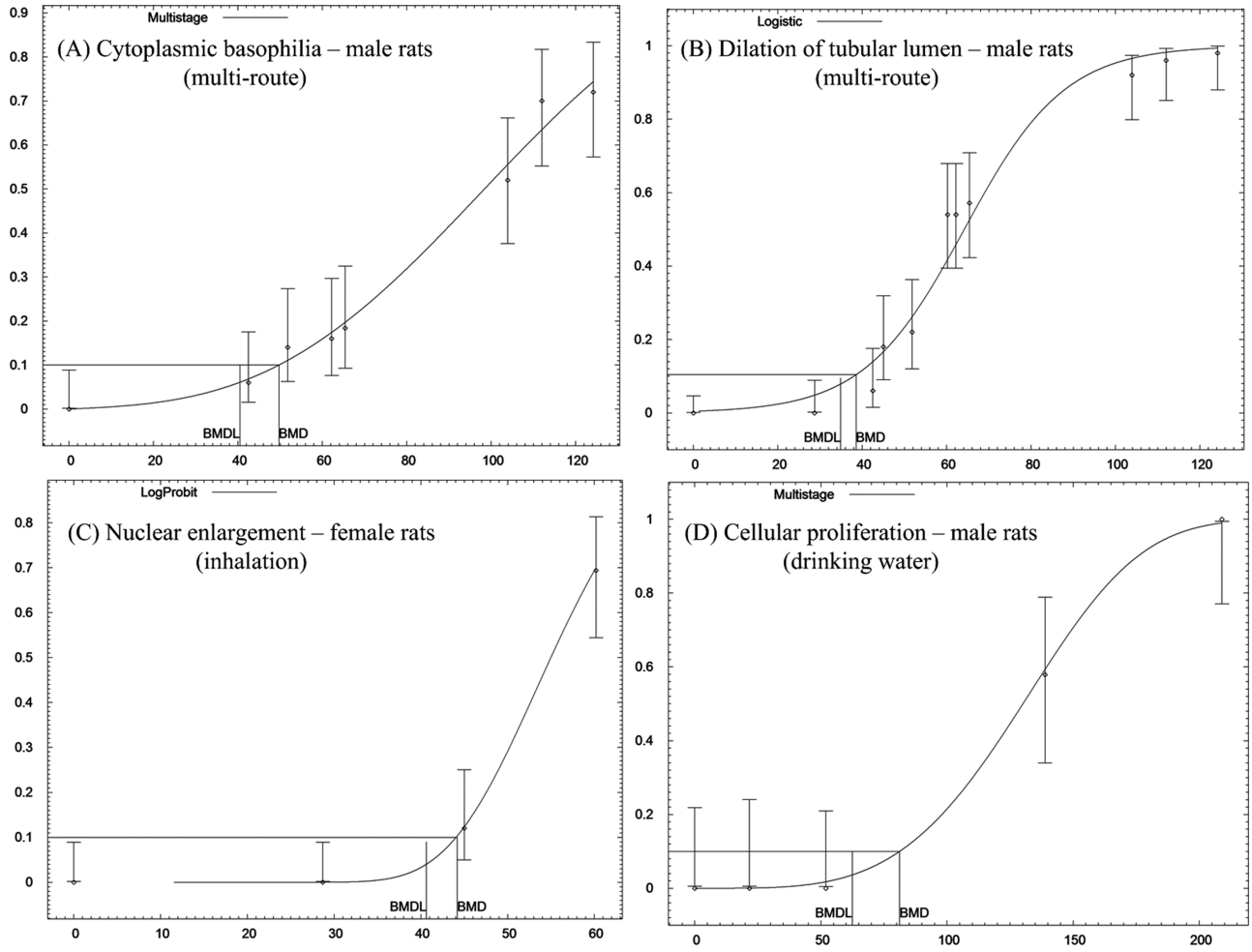

FIG. 8. BMD analysis of multiple endpoints for kidney toxicity in rats using PBPK-derived internal dose metrics. The y-axis is fractional incidence of response, and the x-axis is internal kidney dose (mg/l-24 h). Data points represent response in rats exposed via inhalation, drinking water, or both routes simultaneously based on Yamamoto/Nagano data (Nagano *et al*., 2006; Yamamoto *et al*., 2002) (A–C) and Hard *et al*. (2000) (D). As seen in (A) and (B), the dose-response curve is greatly informed by the inclusion of the simultaneous inhalation + drinking water dose-response data. (A) Cytoplasmic basophilia—male rats (multiroute); (B) dilation of tubular lumen—male rats (multiroute); (C) nuclear enlargement—female rats (inhalation); (D) cellular proliferation—male rats (drinking water).

difference is reduced substantially when assessed by internal dose (Table 7). For a number of endpoints, $BMD_{10}/BMDL_{10}$ was consistent across species, sex, and route of exposure when modeling was conducted using internal doses. This serves as an example of how PBPK modeling can increase confidence in quantitative estimates of site-specific organ toxicity.

Inclusion of the drinking water data by Nagano *et al*. (2006) provided four additional dose groups for dose-response analysis of kidney data for male F344 rats. A monotonically increasing dose-response relationship resulted for most of the endpoints if the multiroute incidence data were incorporated into the analysis (Figs. 7 and 8). Nuclear enlargement was the only endpoint for which the drinking water data were not entirely consistent with the inhalation data, and a reliable BMD/BMDL calculation could not be performed for multiple routes. This may indicate that the PBPK model does not adequately characterize kidney internal dose at extremely high exposures, or there may be toxicodynamic mechanisms that become significant at the high exposure level that are not included in the current model.

PBPK modeling allowed for a consistent analysis of renal toxicity data for chloroform across multiple species and exposure routes. BMD analysis of response data from multiroute exposures was made possible by converting external exposures to a common, site-specific internal dose metric using the revised PBPK model. Incidence of cytoplasmic basophilia, dilation of the tubular lumen, and atypical tubule hyperplasia produced continuous dose-response curves when assessed on a basis of the PBPK-derived internal dose. Furthermore, there was agreement between the doses to the rat and mouse kidneys estimated to cause a 10% response, regardless of the presumed species differences in susceptibility suggested by analysis of just external exposure. The progression of endpoint severity from cytotoxicity to compensatory regeneration is also conserved across species. For the rat, internal $BMDL_{10}$ values for tubular nuclear

TABLE 7
BMD Modeling Results and Interspecies Extrapolation Results for Kidney Toxicity

Endpoint	Study[a]	Species	Route	External[b] BMD_{10}	Internal[c] BMD_{10} (mg/l-24 h)	Internal $BMDL_{10}$ (mg/l-24 h)	HED_{24}[d] (mg/kg-day)	HED[e] (mg/kg-day)	HEC (ppm)
Nuclear enlargement of proximal tubules	Y	Mouse (M)	Inh	5.82 ppm	77.61	61.96	39.85	5.11	1.22
		Rat (F)	Inh	27.18 ppm	44.20	40.65	33.55	4.24	0.79
		Rat (M)	Inh	29.33 ppm	45.02	41.34	33.81	4.27	0.81
	Y+N	Rat (M)	Inh	41.0 ppm	48.99	46.61	35.64	4.49	0.91
			Inh + Oral	N/A[f]	~47[g]	~43[g]	~34.41	~4.34	~0.84
Atypical tubule hyperplasia	Y	Mouse (M)	Inh	19.45 ppm	248.44	128.74	49.24	7.82	2.68
	N	Rat (M)	Inh + Oral	N/A	106.03	96.43	45.81	6.48	1.95
Dilation of the tubular lumen	Y	Rat (F)	Inh	30.14 ppm	45.00	42.07	34.08	4.30	0.82
		Rat (M)	Inh	24.40 ppm	41.52	36.97	32.09	4.08	0.72
	Y+N	Rat (M)	Inh	28.0 ppm	43.60	40.60	33.53	4.24	0.79
			Inh + Oral	N/A	42.02	39.17	32.98	4.18	0.76
Cytoplasmic basophilia	N	Rat (M)	Inh + Oral	N/A	49.71	40.45	33.48	4.23	0.79
Proliferation	H	Rat (M)	Oral	70.43 mg/kg-day	81.21	62.46	39.97	5.14	1.23

[a]Y, Yamamoto (Yamamoto *et al.*, 2002); N, Nagano (Nagano *et al.*, 2006); Y+N, pooled data; H, Hard (Hard *et al.*, 2000). Results derived from overlapping data for the same endpoint have shaded boxes.
[b]External BMD modeling result obtained based on administered dose or concentration in air, without duration adjustments. A more detailed table containing the external BMDL (with/without duration adjustments) is provided as supplementary material.
[c]Internal BMD modeling result obtained based on the internal dose metric predicted by PBPK modeling, while simulating the exposure regimen of the rodents. Results are units of milligrams of chloroform metabolized per liter tissue volume (over a 24-h period).
[d]HED assuming humans intake chloroform in drinking water at a continuous steady rate for 24 h/day.
[e]HED assuming humans intake chloroform in drinking water as bolus events 6 times/day at varying fractions (sum = 1) of the total daily dose.
[f] External BMD not applicable for multiroute analyses.
[g]Results are approximate. Some dose groups removed from BMD analysis.

enlargement and dilation of the tubular lumen (which are markers of tubular injury) fall in the range of 35–45 mg/l-24 h. These are lower than the 60–100 mg/l-24 h range of $BMDL_{10}$ values estimated for tubular hyperplasia and proliferation (which are indicators of proximal tubule regeneration). Similarly for the mouse, the $BMDL_{10}$ for nuclear enlargement is 62 mg/l, whereas the $BMDL_{10}$ for tubular hyperplasia is 129 mg/l.

The improved comparisons were achieved by (1) assuming that the metabolically active region of the kidney was limited to the cortex, (2) determining the MSP content of the mouse kidney cortex *in vitro*, and (3) accounting for differences in MSP content consistently for rats and mice. Only with these revisions do the PBPK modeling and BMD analysis produce consistent internal dose metric values across species. For example, applying the original Corley model to inhalation data for nuclear enlargement produces an internal kidney $BMDL_{10}$ of 80 mg/l in the mouse and 40 mg/l in the rat. Extrapolating to humans (again using the original model) produces HECs of 85 and 18 ppm, respectively. Because the kidney metabolic rate constants of other revised models are similar to those of Corley (see Table 3), those models would also predict inconsistencies. Using the revised model, however, rat and mouse internal dose $BMDL_{10}$ values and the respective HEC values differ by less than 25% for the nuclear enlargement endpoint (Table 7).

Although the revised estimated rate of metabolism in the kidney was decreased by about a factor of 2 in rodents compared with prior publications, it was increased a factor of 2 in humans (Table 3). As a result, the updated model predicted lower HEDs and HECs relative to the older models when using metabolism as the dose metric. Despite this change, the results presented here are plausible and within range of other similar studies. Most notably, Liao *et al*. (2007) employed a PBPK and biologically based dose-response methodology and analyzed labeling index data from assays not incorporated in this work. By cross-species extrapolation, investigators estimated increased kidney toxicity to occur in humans at a continuous inhaled concentration of 0.9 ppm or a continuous oral dose of 30 mg/kg-day (before application of uncertainty factors). Both of these results are in agreement with this study if assuming continuous 24 h/day human exposure. For the cytotoxicity endpoints, the HEC is between 0.7 and 0.9 ppm, and the HED_{24} is between 30 and 40 mg/kg-day. However, the effect of simulating a more realistic drinking water exposure in the human lowered the HED nearly 10-fold. Taken together (well-defined dose-response curves, cross-route/cross-species agreement, and consistency with a prior alternative analysis), there is increased confidence in (1) the PBPK modeling approach, (2) the robustness of using site-specific chloroform metabolism as the internal dose metric, and (3) the database for renal toxicity in rats and mice.

SUPPLEMENTARY DATA

Supplementary data are available online at http://toxsci.oxfordjournals.org/.

FUNDING

No specific source of funding.

ACKNOWLEDGMENTS

We would like to acknowledge Justin Teeguarden and Harish Shankaran for their technical and scientific guidance and Richard Corley for graciously sharing his computational code. We would also like to thank Makoto Take, Seigo Yamamoto, Makoto Ohnishi, Michiharu Matsumoto, Kasuke Nagano, Takashi Hirota, and Shoji Fukushima from the Japan Bioassay Research Center for providing us their pharmacokinetic data. We would also like to thank Cecilia Tan, Ambuja Bale, Lynn Flowers, and Vincent Cogliano for their helpful comments during manuscript preparation.

REFERENCES

Amet, Y., Berthou, F., Fournier, G., Dréano, Y., Bardou, L., Clèdes, J., and Ménez, J. F. (1997). Cytochrome P450 4A and 2E1 expression in human kidney microsomes. *Biochem. Pharmacol.* **53,** 765–771.

Aukland, K. (1976). Renal blood flow. *Int. Rev. Physiol.* **11,** 23–79.

Baker, J. R., Edwards, R. J., Lasker, J. M., Moore, M. R., and Satarug, S. (2005). Renal and hepatic accumulation of cadmium and lead in the expression of CYP4F2 and CYP2E1. *Toxicol. Lett.* **159,** 182–191.

Barger, A., and Herd, J. (1973). Renal vascular anatomy and distribution of blood flow. In *Handbook of Physiology* (J. A. Berliner and R. Orloff, Eds.), pp. 249–313. American Physiological Society, Washington, DC.

Barter, Z. E., Bayliss, M. K., Beaune, P. H., Boobis, A. R., Carlile, D. J., Edwards, R. J., Houston, J. B., Lake, B. G., Lipscomb, J. C., Pelkonen, O. R., et al. (2007). Scaling factors for the extrapolation of in vivo metabolic drug clearance from in vitro data: Reaching a consensus on values of human microsomal protein and hepatocellularity per gram of liver. *Curr. Drug Metab.* **8,** 33–45.

Boorman, G. A. (1999). Drinking water disinfection byproducts: Review and approach to toxicity evaluation. *Environ. Health Perspect.* **107**(Suppl. 1), 207–217.

Brown, B. R., Jr, Sipes, I. G., and Sagalyn, A. M. (1974). Mechanisms of acute hepatic toxicity: Chloroform, halothane, and glutathione. *Anesthesiology* **41,** 554–561.

Brown, R. P., Delp, M. D., Lindstedt, S. L., Rhomberg, L. R., and Beliles, R. P. (1997). Physiological parameter values for physiologically based pharmacokinetic models. *Toxicol. Ind. Health* **13,** 407–484.

Chiu, W. A., Barton, H. A., DeWoskin, R. S., Schlosser, P., Thompson, C. M., Sonawane, B., Lipscomb, J. C., and Krishnan, K. (2007). Evaluation of physiologically based pharmacokinetic models for use in risk assessment. *J. Appl. Toxicol.* **27,** 218–237.

Constan, A. A., Sprankle, C. S., Peters, J. M., Kedderis, G. L., Everitt, J. I., Wong, B. A., Gonzalez, F. L., and Butterworth, B. E. (1999). Metabolism of chloroform by cytochrome P450 2E1 is required for induction of toxicity in the liver, kidney, and nose of male mice. *Toxicol. Appl. Pharmacol.* **160,** 120–126.

Corley, R. A., Mendrala, A. L., Smith, F. A., Staats, D. A., Gargas, M. L., Conolly, R. B., Andersen, M. E., and Reitz, R. H. (1990). Development of a physiologically based pharmacokinetic model for chloroform. *Toxicol. Appl. Pharmacol.* **103,** 512–527.

Cummings, B. S., Lasker, J. M., and Lash, L. H. (2000). Expression of glutathione-dependent enzymes and cytochrome P450s in freshly isolated and

primary cultures of proximal tubular cells from human kidney. *J. Pharmacol. Exp. Ther.* **293,** 677–685.

Cummings, B. S., Parker, J. C., and Lash, L. H. (2001). Cytochrome p450-dependent metabolism of trichloroethylene in rat kidney. *Toxicol. Sci.* **60,** 11–19.

Cummings, B. S., Zangar, R. C., Novak, R. F., and Lash, L. H. (1999). Cellular distribution of cytochromes P-450 in the rat kidney. *Drug Metab. Dispos.* **27,** 542–548.

Davis, J. A., Gift, J. S., and Zhao, Q. J. (2011). Introduction to benchmark dose methods and U.S. EPA's benchmark dose software (BMDS) version 2.1.1. *Toxicol. Appl. Pharmacol.* **254,** 181–191.

Davis, R. R., Murphy, W. J., Snawder, J. E., Striley, C. A., Henderson, D., Khan, A., and Krieg, E. F. (2002). Susceptibility to the ototoxic properties of toluene is species specific. *Hear. Res.* **166,** 24–32.

De Biasi, A., Sbraccia, M., Keizer, J., Testai, E., and Vittozzi, L. (1992). The regioselective binding of CHCl3 reactive intermediates to microsomal phospholipids. *Chem. Biol. Interact.* **85,** 229–242.

Evans, M. V., Boyes, W. K., Simmons, J. E., Litton, D. K., and Easterling, M. R. (2002). A comparison of Haber's rule at different ages using a physiologically based pharmacokinetic (PBPK) model for chloroform in rats. *Toxicology* **176,** 11–23.

Fang, C., Behr, M., Xie, F., Lu, S., Doret, M., Luo, H., Yang, W., Aldous, K., Ding, X., and Gu, J. (2008). Mechanism of chloroform-induced renal toxicity: Non-involvement of hepatic cytochrome P450-dependent metabolism. *Toxicol. Appl. Pharmacol.* **227,** 48–55.

Fry, B. J., Taylor, T., and Hathway, D. E. (1972). Pulmonary elimination of chloroform and its metabolite in man. *Arch. Int. Pharmacodyn. Ther.* **196,** 98–111.

Gemma, S., Ade, P., Sbraccia, M., Testai, E., and Vittozzi, L. (1996a). In vitro quantitative determination of phospholipid adducts of chloroform intermediates in hepatic and renal microsomes from different rodent strains. *Environ. Toxicol. Pharmacol.* **2,** 233–242.

Gemma, S., Faccioli, S., Chieco, P., Sbraccia, M., Testai, E., and Vittozzi, L. (1996b). In vivo CHCl3 bioactivation, toxicokinetics, toxicity, and induced compensatory cell proliferation in B6C3F1 male mice. *Toxicol. Appl. Pharmacol.* **141,** 394–402.

Gemma, S., Testai, E., Chieco, P., and Vittozzi, L. (2004). Bioactivation, toxicokinetics and acute effects of chloroform in Fisher 344 and Osborne Mendel male rats. *J. Appl. Toxicol.* **24,** 203–210.

Gemma, S., Vittozzi, L., and Testai, E. (2003). Metabolism of chloroform in the human liver and identification of the competent P450s. *Drug Metab. Dispos.* **31,** 266–274.

Gopinath, C., and Ford, J. H. (1975). The role of microsomal hydroxylases in the modification of chloroform hepatotoxicity in rats. *Br. J. Exp. Pathol.* **56,** 412–422.

Hard, G. C., Boorman, G. A., and Wolf, D. C. (2000). Re-evaluation of the 2-year chloroform drinking water carcinogenicity bioassay in Osborne-Mendel rats supports chronic renal tubule injury as the mode of action underlying the renal tumor response. *Toxicol. Sci.* **53,** 237–244.

Henderson, C. J., Scott, A. R., Yang, C. S., and Wolf, C. R. (1990). Testosterone-mediated regulation of mouse renal cytochrome P-450 isoenzymes. *Biochem. J.* **266,** 675–681.

Hong, J. Y., Pan, J. M., Ning, S. M., and Yang, C. S. (1989). Molecular basis for the sex-related difference in renal N-nitrosodimethylamine demethylase in C3H/HeJ mice. *Cancer Res.* **49,** 2973–2979.

Jorgenson, T. A., Meierhenry, E. F., Rushbrook, C. J., Bull, R. J., and Robinson, M. (1985). Carcinogenicity of chloroform in drinking water to male Osborne-Mendel rats and female B6C3F1 mice. *Fundam. Appl. Toxicol.* **5,** 760–769.

Kasai, T., Nishizawa, T., Arito, H., Nagano, K., Yamamoto, S., Matsushima, T., and Kawamoto, T. (2002). Acute and subchronic inhalation toxicity of chloroform in rats and mice. *J. Occup. Health* **44,** 193–202.

Larson, J. L., Templin, M. V., Wolf, D. C., Jamison, K. C., Leininger, J. R., Méry, S., Morgan, K. T., Wong, B. A., Conolly, R. B., and Butterworth, B. E. (1996). A 90-day chloroform inhalation study in female and male B6C3F1 mice: Implications for cancer risk assessment. *Fundam. Appl. Toxicol.* **30,** 118–137.

Larson, J. L., Wolf, D. C., and Butterworth, B. E. (1993). Acute hepatotoxic and nephrotoxic effects of chloroform in male F-344 rats and female B6C3F1 mice. *Fundam. Appl. Toxicol.* **20,** 302–315.

Liao, K. H., Tan, Y. M., Conolly, R. B., Borghoff, S. J., Gargas, M. L., Andersen, M. E., and Clewell, H. J., 3rd. (2007). Bayesian estimation of pharmacokinetic and pharmacodynamic parameters in a mode-of-action-based cancer risk assessment for chloroform. *Risk Anal.* **27,** 1535–1551.

Lipscomb, J. C., Barton, H. A., Tornero-Velez, R., Evans, M. V., Alcasey, S., Snawder, J. E., and Laskey, J. (2004). The metabolic rate constants and specific activity of human and rat hepatic cytochrome P-450 2E1 toward toluene and chloroform. *J. Toxicol. Environ. Health Part A* **67,** 537–553.

Lipscomb, J. C., and Kedderis, G. K. (2006). Use of Physiologically Based Pharmacokinetic Models to Quantify the Impact of Human Age and Interindividual Differences in Physiology and Biochemistry Pertinent to Risk (EPA/600/R-06/014A).

Lipscomb, J. C., Teuschler, L. K., Swartout, J., Popken, D., Cox, T., and Kedderis, G. L. (2003). The impact of cytochrome P450 2E1-dependent metabolic variance on a risk-relevant pharmacokinetic outcome in humans. *Risk Anal.* **23,** 1221–1238.

Lohr, J. W., Willsky, G. R., and Acara, M. A. (1998). Renal drug metabolism. *Pharmacol. Rev.* **50,** 107–141.

Luke, N. S., Sams, R., 2nd, DeVito, M. J., Conolly, R. B., and El-Masri, H. A. (2010). Development of a quantitative model incorporating key events in a hepatotoxic mode of action to predict tumor incidence. *Toxicol. Sci.* **115,** 253–266.

Meek, M. E., Beauchamp, R., Long, G., Moir, D., Turner, L., and Walker, M. (2002). Chloroform: Exposure estimation, hazard characterization, and exposure-response analysis. *J. Toxicol. Environ. Health. B. Crit. Rev.* **5,** 283–334.

Mohla, S., Ahir, S., and Ampy, F. R. (1988). Tissue specific regulation of renal N-nitrosodimethylamine-demethylase activity by testosterone in BALB/c mice. *Biochem. Pharmacol.* **37,** 2697–2702.

Nagano, K., Kano, H., Arito, H., Yamamoto, S., and Matsushima, T. (2006). Enhancement of renal carcinogenicity by combined inhalation and oral exposures to chloroform in male rats. *J. Toxicol. Environ. Health Part A* **69,** 1827–1842.

Navar, L., Evan, A., and Rosivall, L. (1983). Microcirculation of the kidneys. In *The Physiology and Pharmacology of the Microcirculation*, Vol. 1, pp. 397–488. Academic Press, New York.

Noort, D., Hulst, A. G., Fidder, A., van Gurp, R. A., de Jong, L. P., and Benschop, H. P. (2000). In vitro adduct formation of phosgene with albumin and hemoglobin in human blood. *Chem. Res. Toxicol.* **13,** 719–726.

Palmer, A. K., Street, A. E., Roe, F. J., Worden, A. N., and Van Abbé, N. J. (1979). Safety evaluation of toothpaste containing chloroform. II. Long term studies in rats. *J. Environ. Pathol. Toxicol.* **2,** 821–833.

Pereira, M. A., and Chang, L. W. (1981). Binding of chemical carcinogens and mutagens to rat hemoglobin. *Chem. Biol. Interact.* **33,** 301–305.

Pereira, M. A., Chang, L. W., Ferguson, J. L., and Couri, D. (1984). Binding of chloroform to the cysteine of hemoglobin. *Chem. Biol. Interact.* **51,** 115–124.

Philip, B. K., Anand, S. S., Palkar, P. S., Mumtaz, M. M., Latendresse, J. R., and Mehendale, H. M. (2006). Subchronic chloroform priming protects mice from a subsequently administered lethal dose of chloroform. *Toxicol. Appl. Pharmacol.* **216,** 108–121.

Pohl, L. R., Branchflower, R. V., Highet, R. J., Martin, J. L., Nunn, D. S., Monks, T. J., George, J. W., and Hinson, J. A. (1981). The formation of diglutathionyl dithiocarbonate as a metabolite of chloroform, bromotrichloromethane, and carbon tetrachloride. *Drug Metab. Dispos.* **9,** 334–339.

Riederer, A. M., Bartell, S. M., and Ryan, P. B. (2009). Predictors of personal air concentrations of chloroform among US adults in NHANES 1999-2000. *J. Expo. Sci. Environ. Epidemiol.* **19,** 248–259.

Roe, F. J., Palmer, A. K., Worden, A. N., and Van Abbé, N. J. (1979). Safety evaluation of toothpaste containing chloroform. I. Long-term studies in mice. *J. Environ. Pathol. Toxicol.* **2,** 799–819.

Roy, A., Weisel, C. P., Lioy, P. J., and Georgopoulos, P. G. (1996). A distributed parameter physiologically-based pharmacokinetic model for dermal and inhalation exposure to volatile organic compounds. *Risk Anal.* **16,** 147–160.

Schoeny, R., Haber, L., and Dourson, M. (2006). Data considerations for regulation of water contaminants. *Toxicology* **221,** 217–224.

Smith, J. H., and Hook, J. B. (1983). Mechanism of chloroform nephrotoxicity. II. In vitro evidence for renal metabolism of chloroform in mice. *Toxicol. Appl. Pharmacol.* **70,** 480–485.

Smith, J. H., and Hook, J. B. (1984). Mechanism of chloroform nephrotoxicity. III. Renal and hepatic microsomal metabolism of chloroform in mice. *Toxicol. Appl. Pharmacol.* **73,** 511–524.

Snawder, J. E., and Lipscomb, J. C. (2000). Interindividual variance of cytochrome P450 forms in human hepatic microsomes: Correlation of individual forms with xenobiotic metabolism and implications in risk assessment. *Regul. Toxicol. Pharmacol.* **32,** 200–209.

Spiteri, N. J. (1982). Circadian patterning of feeding, drinking and activity during diurnal food access in rats. *Physiol. Behav.* **28,** 139–147.

Take, M., Yamamoto, S., Ohnishi, M., Matsumoto, M., Nagano, K., Hirota, T., and Fukushima, S. (2010). Chloroform distribution and accumulation by combined inhalation plus oral exposure routes in rats. *J. Environ. Sci. Health. A. Tox. Hazard. Subst. Environ. Eng.* **45,** 1616–1624.

Tan, Y. M., Butterworth, B. E., Gargas, M. L., and Conolly, R. B. (2003). Biologically motivated computational modeling of chloroform cytolethality and regenerative cellular proliferation. *Toxicol. Sci.* **75,** 192–200.

Templin, M. V., Constan, A. A., Wolf, D. C., Wong, B. A., and Butterworth, B. E. (1998). Patterns of chloroform-induced regenerative cell proliferation in BDF1 mice correlate with organ specificity and dose-response of tumor formation. *Carcinogenesis* **19,** 187–193.

Templin, M. V., Jamison, K. C., Sprankle, C. S., Wolf, D. C., Wong, B. A., and Butterworth, B. E. (1996a). Chloroform-induced cytotoxicity and regenerative cell proliferation in the kidneys and liver of BDF1 mice. *Cancer Lett.* **108,** 225–231.

Templin, M. V., Larson, J. L., Butterworth, B. E., Jamison, K. C., Leininger, J. R., Méry, S., Morgan, K. T., Wong, B. A., and Wolf, D. C. (1996b). A 90-day chloroform inhalation study in F-344 rats: Profile of toxicity and relevance to cancer studies. *Fundam. Appl. Toxicol.* **32,** 109–125.

Testai, E., De Curtis, V., Gemma, S., Fabrizi, L., Gervasi, P., and Vittozzi, L. (1996). The role of different cytochrome P450 isoforms in in vitro chloroform metabolism. *J. Biochem. Toxicol.* **11,** 305–312.

Testai, E., Di Marzio, S., and Vittozzi, L. (1990). Multiple activation of chloroform in hepatic microsomes from uninduced B6C3F1 mice. *Toxicol. Appl. Pharmacol.* **104,** 496–503.

U.S. EPA. (2012). Benchmark Dose Technical Guidance. Risk Assessment Forum, Washington, DC; EPA/100/R-12/001. Available at: http://www.epa.gov/raf/publications/benchmarkdose.htm

Vittozzi, L., Gemma, S., Sbraccia, M., and Testai, E. (2000). Comparative characterization of CHCl(3) metabolism and toxicokinetics in rodent strains differently susceptible to chloroform-induced carcinogenicity. *Environ. Toxicol. Pharmacol.* **8,** 103–110.

WHO. (2005). Trihalomethanes in Drinking-water: Background document for development of WHO Guidelines for Drinking-water Quality. *WHO/SDE/WSH/03.04/64*. World Health Organization, Geneva.

Yamamoto, S., Kasai, T., Matsumoto, M., Nishizawa, T., Arito, H., Nagano, K., and Matsushima, T. (2002). Carcinogenicity and chronic toxicity in rats and mice exposed to chloroform by inhalation. *J. Occup. Health* **44,** 283–293.

Yamamoto, S., Nishizawa, T., Nagano, K., Aiso, S., Kasai, T., Takeuchi, T., and Matsushima, T. (1999). Development of resistance to chloroform toxicity in male BDF1 mice exposed to a stepwise increase in chloroform concentration. *J. Toxicol. Sci.* **24,** 421–424.

Yoon, M., Madden, M. C., and Barton, H. A. (2007). Extrahepatic metabolism by CYP2E1 in PBPK modeling of lipophilic volatile organic chemicals: Impacts on metabolic parameter estimation and prediction of dose metrics. *J. Toxicol. Environ. Health Part A* **70,** 1527–1541.

Zerilli, A., Lucas, D., Amet, Y., Beauge, F., Volant, A., Floch, H. H., Berthou, F., and Menez, J. F. (1995). Cytochrome P-450 2E1 in rat liver, kidney and lung microsomes after chronic administration of ethanol either orally or by inhalation. *Alcohol Alcohol.* **30,** 357–365.